

Autoinhibition of X11/Mint scaffold proteins revealed by the closed conformation of the PDZ tandem

Jia-Fu Long¹, Wei Feng¹, Rui Wang, Ling-Nga Chan, Fanny C F Ip, Jun Xia, Nancy Y Ip & Mingjie Zhang

Members of the X11/Mint family of multidomain adaptor proteins are composed of a divergent N terminus, a conserved PTB domain and a pair of C-terminal PDZ domains. Many proteins can interact with the PDZ tandem of X11 proteins, although the mechanism of such interactions is unclear. Here we show that the highly conserved C-terminal tail of X11 α folds back and inserts into the target-binding groove of the first PDZ domain. The binding of this tail occludes the binding of other target peptides. This autoinhibited conformation of X11 requires that the two PDZ domains and the entire C-terminal tail be covalently connected to form an integral structural unit. The autoinhibited conformation of the X11 PDZ tandem provides a mechanistic explanation for the unique target-binding properties of the protein and hints at potential regulatory mechanisms for the X11–target interactions.

The X11/Mint family of multidomain scaffold proteins comprises three members: X11 α /Mint1, X11 β /Mint2 and X11 γ /Mint3 (refs. 1–5). X11 α /Mint1 and X11 β /Mint2 are neuron-specific proteins, whereas X11 γ /Mint3 is ubiquitously expressed^{2,6–9}. Except for their isoform-specific N-terminal sequences, all X11/Mint proteins contain a central PTB domain and two C-terminal PDZ domains arranged in tandem (Fig. 1a). The PTB domain binds to the C-terminal YENPTY motif of amyloid precursor protein (APP). This interaction prolongs the half-life of cellular APP, thereby slowing the production of amyloid- β peptide^{3,10–13}. A growing number of proteins that bind to the PDZ domains of X11/Mint proteins have been identified, including presenilin^{13,14}, calcium channels¹⁵, neuexin⁵ and AMPA receptors¹⁶. Although not directly involved in binding APP, the PDZ tandem of X11/Mint proteins has an indispensable role in PTB domain-mediated APP stabilization^{13,17}. Available experimental data indicate that the binding of target proteins to isolated PDZ domains is distinctly different from the binding of those targets to two PDZ domains connected in tandem^{13,14}. Current understanding of the structural and biochemical properties of the X11 PDZ domains cannot explain their unique target-binding properties.

X11/Mint proteins are also implicated in polarized trafficking of receptors and ion channels to plasma membranes^{18–20}. In *Caenorhabditis elegans*, mutation of *lin-10* (the only X11/Mint homolog in *C. elegans*) results in mislocalization of the epidermal growth factor receptor, LET-23, and causes a signaling-defective (vulvaless) phenotype^{18,20}. The proper localization of LET-23 requires an evolutionary conserved complex of LIN-2, LIN-7 and LIN-10 (CASK, Mals and X11 α in mammals)²¹. Mutation of *lin-10* also disrupts postsynaptic targeting of glutamate receptor-1 in *C. elegans* neurons¹⁹. X11 α /Mint1 has been implicated in the kinesin-mediated transport of NMDA receptors to synapses^{22,23} and is preferentially expressed in inhibitory

neurons²⁴. Deletion of X11 α /Mint1 in mice impairs GABAergic synaptic transmission²⁴. That X11 α /Mint1 knockout study, however, argues against the involvement of the protein in the synaptic trafficking of the NMDA receptor, as the X11 α /Mint1-deficient mice showed no alterations in the ratio of AMPA receptor- to NMDA receptor-mediated synaptic currents²⁴.

In this study, we determined the three-dimensional (3D) structures of the isolated PDZ domains of X11 α /Mint1 (referred to from now on as X11 α) by NMR spectroscopy. We uncovered an autoinhibited conformation of the PDZ domains that is mediated by an intramolecular interaction between the conserved C-terminal tail and the first PDZ domain of the X11 α PDZ tandem. Our biochemical data suggest that the interaction between the C-terminal tail and the PDZ domains has a regulatory role in the function of the X11/Mint scaffold proteins.

RESULTS

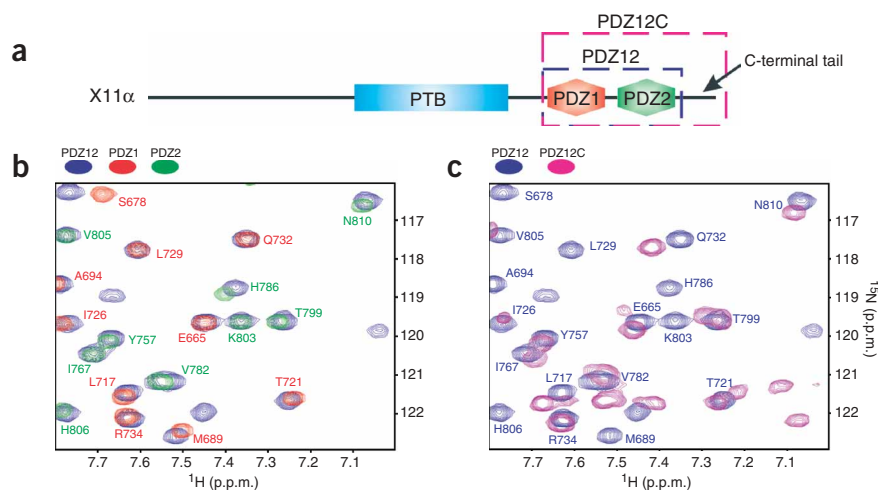
The C terminus of X11 α binds to the PDZ tandem

Earlier biochemical studies indicated that the PDZ tandem of X11 α has target-binding properties that are distinct from those of the individual PDZ domains^{13,14}. It is difficult to conceptualize why binding of a single C terminus requires two PDZ domains. As a first step in understanding X11 PDZ tandem-mediated target recognition, we compared ¹H, ¹⁵N heteronuclear single quantum coherence (HSQC) spectra of the isolated PDZ1 (red, Fig. 1b) and PDZ2 (green) domains and the two covalently connected PDZ domains without the 16-residue C-terminal tail (PDZ12; blue). The summation spectrum of PDZ1 and PDZ2 was highly similar to that of PDZ12. Small differences in chemical shift were observed between the isolated PDZ domains and their tandem form for a few residues outside of their respective conventional C-terminal peptide-binding pockets (the α B

Department of Biochemistry, Molecular Neuroscience Center, Hong Kong University of Science and Technology, Clear Water Bay, Kowloon, Hong Kong, China. ¹These authors contributed equally to this work. Correspondence should be addressed to M.Z. (mzhang@ust.hk).

Published online 10 July 2005; doi:10.1038/nsmb958

Figure 1 The C-terminal tail of X11 α directly interacts with the PDZ tandem. **(a)** Schematic diagram of the domain organization of X11 α . The various forms of PDZ domains used in this study are indicated. **(b)** Superposition plot of ^1H , ^{15}N HSQC spectra of PDZ1, PDZ2 and PDZ1 and PDZ2 in tandem (PDZ12). The summation spectrum of PDZ1 and PDZ2 was essentially the same as the spectrum of PDZ12. **(c)** Superposition plot of the HSQC spectra of PDZ12 and PDZ12C with C-terminal tail (PDZ12C), showing gross differences between the two spectra. For clarity, only a selected region of each spectrum is shown. The chemical shift assignments for PDZ1 and PDZ2 are labeled.



helix, βB strand and $\beta\text{A}/\beta\text{B}$ loop). We concluded that the two PDZ domains in PDZ12 are largely independent of each other. In contrast, the HSQC spectrum of PDZ12 containing the C-terminal tail (PDZ12C, **Fig. 1c**) was distinctly different from that of PDZ12. These data indicate that the C-terminal tail of X11 α interacts directly with the PDZ domains of the protein.

The X11 α PDZ tandem adopts a closed conformation

The last three amino acids of X11 α (Val-Tyr-Ile) resemble a typical PDZ domain binding motif^{25,26}. It seemed possible that the interaction observed in **Figure 1** was mediated by direct binding of the C-terminal tail to one of the PDZ domains in X11 α . To test this hypothesis, we titrated PDZ1 and PDZ2 with a synthetic peptide comprising the last nine amino acids of X11 α (referred to as the C-peptide). The C-peptide interacted with both PDZ domains (**Supplementary Fig. 1** online). The spectrum of PDZ1 saturated with the C-peptide (red, **Fig. 2a** and **Supplementary Fig. 1**) overlapped with a

subset of the peaks from the PDZ12C spectrum (blue). The amino acids in the $\alpha\text{B}/\beta\text{B}$ groove of PDZ1 underwent particularly evident C-peptide-induced chemical shift changes (**Supplementary Fig. 1**). Additionally, the chemical shifts of the isolated PDZ2 and the domain in PDZ12C are highly similar (**Fig. 2a** and **Supplementary Fig. 1**). These observations indicate that the C-terminal tail of X11 α binds to the PDZ1 target-binding pocket in the intact protein, while the target-binding pocket of PDZ2 remains open. This is supported by the observation that a peptide comprising the last ten residues of kinesin motor KIF17 (SKSNFGSEPL)²² induced chemical shift changes limited to PDZ2 (**Fig. 2b**).

We used two different approaches to distinguish whether the observed interaction between PDZ1 and the C-terminal tail of X11 α occurred by an intermolecular or an intramolecular mode. First, we analyzed the molecular masses of PDZ12C and the isolated PDZ domains

using analytical gel filtration chromatography ($\sim 1\text{--}5\text{ mg ml}^{-1}$ of protein). PDZ12C was eluted at a volume indicative of its being a monomer (**Fig. 2c**), suggestive of an intramolecular interaction between

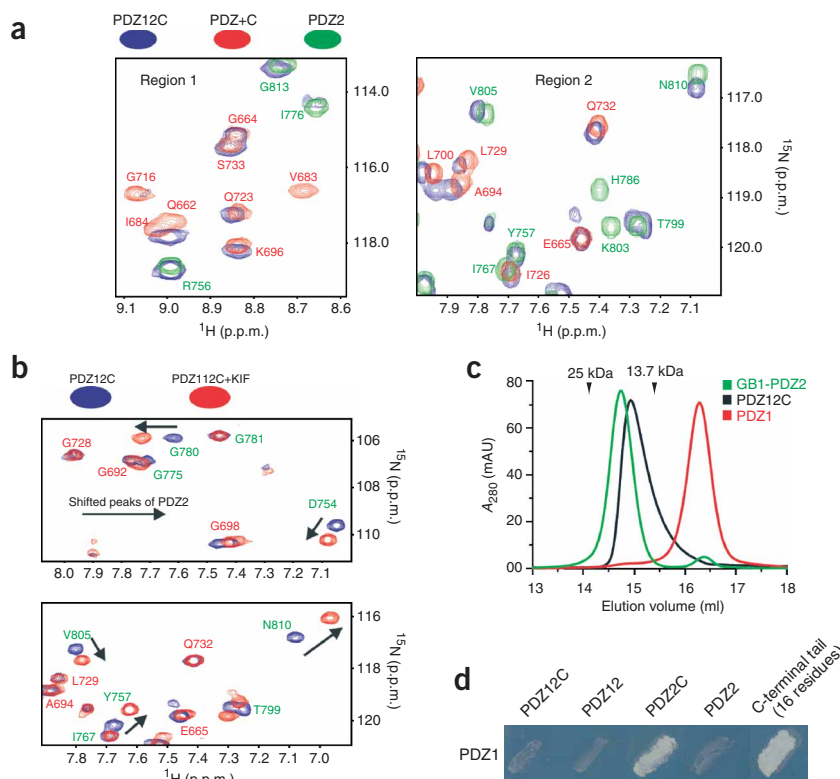


Figure 2 The C-terminal tail of X11 α folds back to PDZ1 to form an autoinhibited conformation. **(a)** Superposition plot of the HSQC spectra of PDZ12C, PDZ1 in complex with C-peptide (PDZ1+C) and PDZ2. The peaks from PDZ1+C overlapped with a subset of peaks from PDZ12C. For clarity, only selected regions of each spectrum are shown. The chemical shift assignments for PDZ1 and PDZ2 are labeled. **(b)** Superposition plot of two selected regions of the HSQC spectra of PDZ12C and PDZ12C with an excess of synthetic KIF17 PDZ-binding peptide (PDZ12C+KIF). The arrows indicate peptide-induced chemical shift changes in peaks from PDZ2. **(c)** Analytical gel filtration analysis of PDZ1, GB1-PDZ2 and PDZ12C. The elution volumes of molecular mass standards are indicated at the top of the panel. The calculated molecular masses for PDZ1, GB1-PDZ2 (after subtracting the mass of the GB1-His₆ fusion tag) and PDZ12C were $\sim 12\text{ kDa}$, $\sim 9.9\text{ kDa}$ and $\sim 20\text{ kDa}$, respectively. **(d)** Yeast two-hybrid assay showing the interactions between PDZ1 and various domains of PDZ12C.

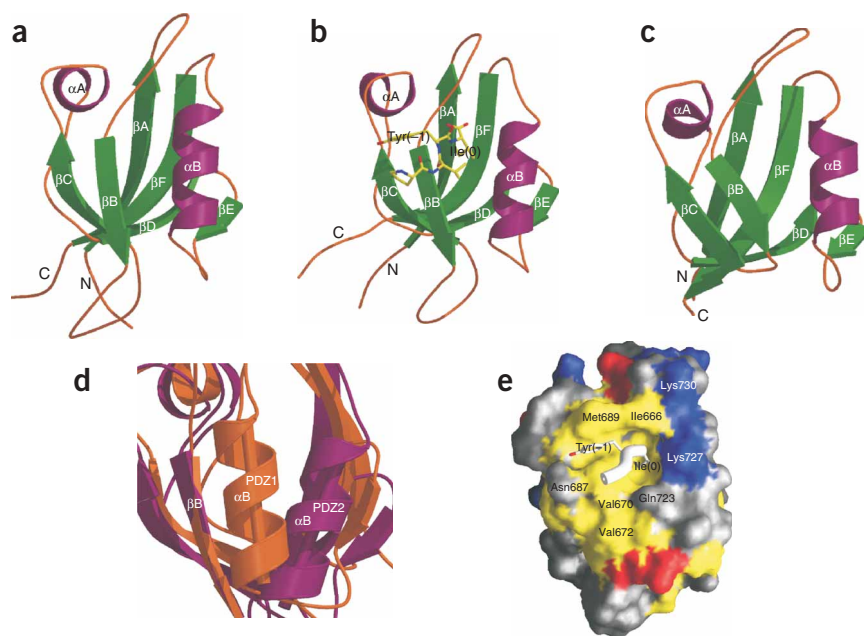


Figure 3 Structures of the X11 α PDZ domains determined by NMR spectroscopy. (a–c) Ribbon diagrams of representative NMR structures of PDZ1 (a), PDZ1 in complex with C-peptide (b) and PDZ2 (c). The C-peptide in b is shown as an explicit atomic model. (d) Comparison of the α B/ β B groove conformation in PDZ1 (orange) and PDZ2 of PSD-95 (purple). The two PDZ domains were superimposed on each other using their respective β B strands. The axis of the α B helix in each PDZ domain is indicated by a solid rod at the center of the helical cylinder. (e) Surface representation of the PDZ1–C-peptide complex. PDZ1 is shown as a surface model, the backbone of the C-peptide is shown as a white worm, and the side chains of the last two residues of the C-peptide are shown as explicit atomic models. The hydrophobic residues of the surface model are shown in yellow, the positively charged residues in blue, the negatively charged residues in red and the rest of amino acids in gray.

PDZ1 and the C-terminal tail. Second, we found using a yeast two-hybrid assay that PDZ1 binds to the C-terminal tail (Fig. 2d), consistent with the NMR experiment. A positive interaction between PDZ1 and PDZ2C (PDZ2 containing the C-terminal tail) was also observed. The negative interaction between PDZ1 and PDZ12C indicated that the stronger intramolecular interaction between the tail and PDZ1 prevented intermolecular binding between the two (Fig. 2d). Control experiments confirmed that PDZ1 interacted with neither PDZ2 nor PDZ12. Taken together, the NMR and biochemical experiments show that the C-terminal tail of X11 α folds back and binds to the PDZ1 domain, resulting in an autoinhibited conformation of the X11 α PDZ tandem.

PDZ1 has a distinct target-binding mode

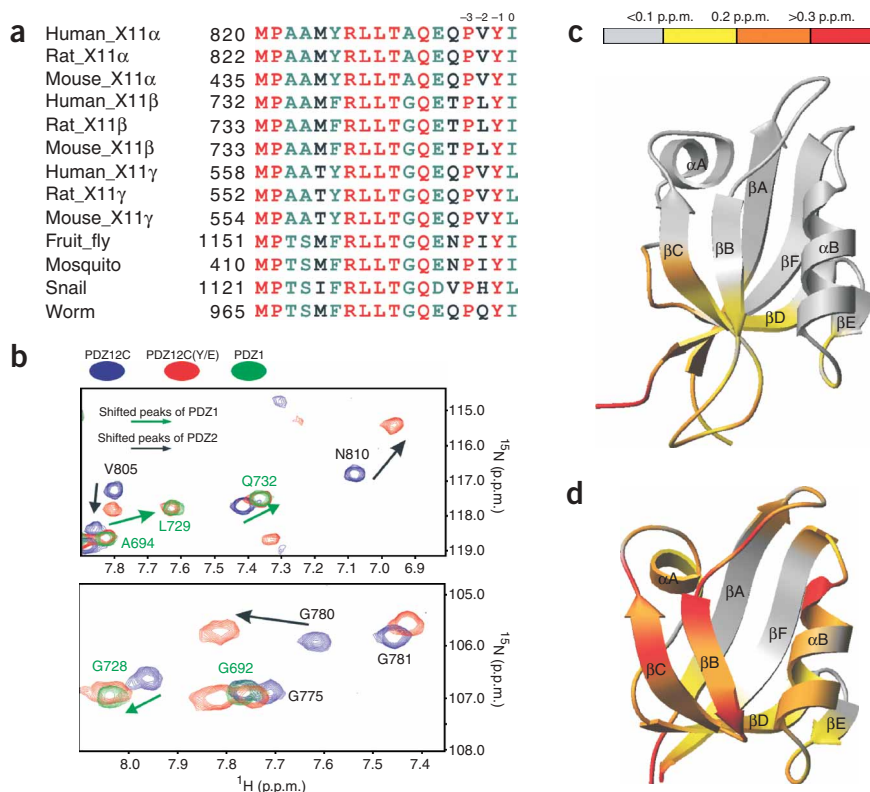
Amino acid sequence analysis suggests that both PDZ1 and PDZ2 have the potential to interact with C-terminal peptides (including the C-terminal tail of X11 itself) containing the sequence Ψ -X- Ψ^* , where Ψ represents hydrophobic amino acids and Ψ^* represents the carboxyl group^{25–27}. However, our data indicated that the C-terminal tail of X11 α binds preferentially to PDZ1 in PDZ12C. To understand the binding specificity of the C-terminal tail and the PDZ domains of X11 α , we determined the 3D structures of the isolated PDZ1 and PDZ2 domains and the PDZ1 domain in complex with the C-peptide (Fig. 3, Supplementary Fig. 2 and Supplementary Table 1 online). Fusion of the B1 domain of streptococcal protein G (GB1) to the N-terminal end of PDZ2 was necessary to overcome the low solubility and poor sample homogeneity of the untagged PDZ2. The structure of PDZ2 was thus determined with GB1 covalently attached to its N-terminus.

Both PDZ1 and PDZ2 have a typical PDZ fold composed of a six-stranded β -barrel with each of its open sides capped by an α -helix (Fig. 3a–c). Detailed analysis, however, revealed marked differences between the two structures. The structures of PDZ1 and PDZ2 also have several unique features that are not present in other PDZ domains with known structures. The conformation of the α B/ β B groove of PDZ1 is radically different from that of PDZ2 and other known C-terminal peptide-binding PDZ domains. In canonical PDZ domains, the β B strand and the α B helix form a V-shaped groove into which the backbone of a C-terminal peptide fits snugly to form an

antiparallel β -sheet with the β B strand. The carboxyl group and the bulky hydrophobic side chain of the last residue of the ligand peptide fill the pockets at the open end of the V-shaped groove (refs. 26–28; see Fig. 3b for an example). In contrast, β B and α B of PDZ1 are antiparallel to each other, and the space between them is too narrow to accommodate the formation of an antiparallel β -sheet of a ligand peptide with β B (Fig. 3a,d). In contrast to this structure-based analysis, the experiments we described earlier showed that the PDZ1 domain binds specifically to the C-terminal tail both as a part of the native protein and as an isolated peptide. This apparent contradiction suggests that PDZ1 of X11 α binds to its target peptide through an unconventional mechanism.

The structure of the PDZ1–C-peptide complex indeed reveals a unique binding mechanism (Fig. 3b,e). Rather than assuming the conformation of a β -strand antiparallel to β B of PDZ1, the C-peptide does not adopt any regular secondary structure in the complex. Instead, the C-terminal end of the peptide inserts itself, in a near-perpendicular orientation, into a pocket formed by the GLGF loop, the end of α B and the loop connecting α B and β F (Fig. 3e). Only the last two amino acid residues of the C-peptide (Tyr836 and Ile837) and the carboxyl group are directly involved in PDZ1 binding. The formation of hydrogen bonds between the C-terminal carboxyl group and the backbone amides in the GLGF loop, as well as the hydrophobic interactions between the side chain of Ile837 from the C-peptide with the side chains of Leu667, Val669 and Ile726 from PDZ1, closely resemble the canonical interaction mode observed in complexes formed between PDZ domain and C-terminal peptide complexes. The extensive interactions between the penultimate Tyr836 of the C-peptide and the direct involvement of α A of the PDZ domain in target binding distinguish X11 α PDZ1 from canonical PDZ domains. The phenyl ring of Tyr836 extends into the β C/ α A loop and fits snugly into a hydrophobic pocket formed by Ile666, Met689 and Val670. The structure of the PDZ1–C-peptide complex indicates that Ile837 and Tyr836 at the extreme C-terminal end have a crucial role in the formation of the complex. NMR titration showed that a mutant C-peptide in which Tyr836 was substituted with glutamate had no detectable binding to PDZ1. In contrast, substitution of Val835 with glutamate did not change the binding of the C-peptide to PDZ1 (data not shown). We also tested the binding of a number of peptides to PDZ1 and found that a hydrophobic residue at the –1 position of

Figure 4 The autoinhibited conformation of PDZ12C might be regulated. (a) Amino acid sequence alignment of the C-terminal tails of various X11 family members. Absolutely conserved amino acids are shown in red, highly conserved residues in green and moderately conserved residues in black. (b) Superposition plot of the HSQC spectra of PDZ12C, the mutant PDZ12(Y/E) and PDZ1. The mutation of Tyr(-1) to Glu released the autoinhibited conformation of PDZ12C. The green arrows indicate the movement of PDZ1 peaks from the ligand-bound form in PDZ12C to the open form in PDZ12C(Y/E); the black arrows indicate the movement of PDZ2 peaks from the open to the ligand-bound form. (c) Summary of the backbone amide chemical shift differences, mapped onto the 3D structure of PDZ1, between isolated PDZ1 and PDZ1 in PDZ12C(Y/E). (d) Summary of chemical shift differences between the ligand-free form of PDZ2 and PDZ2 in PDZ12C(Y/E). The combined ^1H and ^{15}N chemical shift changes were used to characterize the mutation-induced conformational changes of the protein.



the peptide ligands was absolutely required for PDZ1-peptide complex formation (data not shown).

We next investigated the interaction between PDZ1 and a synthetic peptide comprising the C-terminal tail of the N-type voltage-gated calcium channel (HHPDQDHW). PDZ1 bound to the calcium channel peptide and to the C-peptide in a very similar manner (**Supplementary Fig. 3** online). We concluded that peptides with two C-terminal hydrophobic residues have the potential to bind to the isolated PDZ1 domain through the binding mode observed for the complex of PDZ1 and C-peptide (**Fig. 3b**). However, such binding is not likely to occur in intact X11 α , as the peptide-binding pocket of PDZ1 is occupied by its own C terminus through a stronger intramolecular interaction.

The amino acid sequence of PDZ2 is unusually short (80 residues) compared to those of most PDZ domains (typically 90–100 residues). The loop connecting the βB and βC strands contains only one residue (Gly766), and the βB and βC strands and the αB helix are shorter than the corresponding segments in most other known PDZ structures (**Fig. 3c**). As a result, the C-terminal peptide-binding groove of PDZ2 can accommodate no more than three amino acids, as compared to four to seven residues for most PDZ domains^{26,29}. The structure of the X11 α PDZ2 resembles that of the second PDZ domain of the syntenin, which was recently characterized³⁰. An analysis of chemical shift perturbation revealed that the isolated C-peptide binds to PDZ2 by a canonical mode (data not shown).

PDZ12C functions as an integral structural unit

The simplest explanation for the autoinhibited conformation of PDZ12C is that the C-peptide has a higher binding affinity for PDZ1 than for PDZ2. To verify this, we measured the dissociation constants of the C-peptide under various conditions. Unexpectedly, PDZ1 had an approximately five-fold weaker binding affinity for the isolated C-peptide than did PDZ2 ($93.8 \pm 5.8 \mu\text{M}$ versus $20.1 \pm 3.1 \mu\text{M}$). In addition, both PDZ1 and PDZ2 bound to the isolated C-peptide with relatively low affinities. These data indicate that the PDZ12 tandem, in the context of PDZ12C, not only enhances the

binding affinity of the covalently connected C-terminal tail for the PDZ domains but also leads to the specific binding of the C-terminal tail to PDZ1.

The amino acid sequences of the C-terminal tails of the X11 proteins are highly conserved, and residues between PDZ2 and the PDZ-binding motif are highly hydrophobic (**Fig. 4**). Extending PDZ12 by including this stretch of hydrophobic amino acids (residues 655–829; referred to as PDZ12E) substantially altered the binding affinity of the PDZ tandem for the C-peptide ($K_d = 9.2 \pm 0.6 \mu\text{M}$, versus $16 \pm 1.2 \mu\text{M}$ for PDZ12), indicating that these hydrophobic residues interact with the PDZ tandem and influence its target-binding properties.

We tried to use a synthetic peptide containing the entire 16-residue C-terminal tail to study its interaction with the PDZ domains of X11. However, our attempt was unsuccessful because of the extremely low solubility of the peptide. Nevertheless, the interaction between the tail and the PDZ tandem in PDZ12C was inferred by comparing the HSQC spectra of the various forms of PDZ domains used in this study (**Fig. 5**). In this analysis, the chemical shift changes of both PDZ domains as a result of each step of construct change were mapped onto the PDZ domain structures. PDZ1 and PDZ2 are linked by the conserved four-residue fragment Cys-Pro-Pro-Val. This short segment brings the two domains close together and induces some interaction between the two domains, as indicated by the linker-induced chemical shift changes. The residues that showed shift differences were concentrated in the regions in the vicinity of the linker sequence, away from the respective target-binding pockets of the two PDZ domains (**Fig. 5b**). The relatively small chemical shift changes suggested that the interaction of the two PDZ domains in PDZ12 is transient. The inclusion of the stretch of conserved hydrophobic amino acids immediately following PDZ2 (that is, PDZ12E) induced further chemical shift changes in a number of residues from both PDZ1

and PDZ2 (Fig. 5b,c), indicating that this hydrophobic stretch indeed interacts with the PDZ tandem. In addition, the chemical shift changes induced by extending PDZ12 to PDZ12E were located in the interface between PDZ1 and PDZ2, suggesting that this hydrophobic extension interacts physically with the interface. Further extension of PDZ12E by inclusion of the rest of the C-terminal tail induced substantial chemical shift changes to PDZ1 only (Fig. 5c,d), indicating that the tail specifically binds to PDZ1. It is probable that the stretch of hydrophobic residues between PDZ2 and the C-terminal PDZ-binding motif, together with PDZ2, guides the C-terminal tail to PDZ1. Taken together, our NMR and biochemical studies show that the two PDZ domains and the entire C-terminal tail of X11 α function as an integral structural unit.

The closed conformation of X11 α could be regulated

The PDZ-binding motif of the PDZ12C contains an absolutely conserved Tyr(-1) residue (Fig. 4a), suggesting that the interaction between PDZ1 and the C terminus of X11 α is regulated by phosphorylation of Tyr(-1). Substitution of Tyr(-1) with glutamate in the C-peptide abolished its binding capability to PDZ1, but it is not known whether mutation of Tyr(-1) in PDZ12C would also release the autoinhibition of PDZ1. To test this, we changed Tyr(-1) in PDZ12C to glutamate (PDZ12C(Y/E)) and compared the conformation of that mutant with that of the wild-type protein. Substitution of Tyr(-1) resulted in overall spectral changes (compare blue and red, Fig. 4b), suggesting that both PDZ1 and PDZ2 underwent mutation-induced conformational changes. The peaks in the spectrum of free PDZ1 (green) nearly overlapped with a subset of peaks in the spectrum of the PDZ12C(Y/E) mutant (Fig. 4b), indicating that the PDZ1 domain in PDZ12C(Y/E) adopted an open conformation. This conformation was visualized by mapping the chemical shift differences between free PDZ1 and PDZ12C(Y/E) to the 3D structure of the domain (Fig. 4c).

In contrast, the spectrum of free PDZ2 did not overlap with any subset of the peaks from the spectrum of PDZ12C(Y/E) (compare Figs. 1 and 4b), indicating that the PDZ2 domain underwent marked conformational changes as a result of the mutation. The mutation induced large chemical shift changes to the ligand-binding pocket (the α B/ β B groove) of PDZ2 (Fig. 4d), indicating that the C-terminal tail of the PDZ12C(Y/E) bound to PDZ2. Consistent with this notion, peaks from the HSQC spectrum of PDZ2 saturated with the mutant C-peptide largely overlapped with a subset of peaks in the HSQC spectrum of the PDZ12C(Y/E) mutant (data not shown). Taken together, the data in Figure 4 show that mutation of Tyr(-1) to glutamate releases the C-terminal tail from PDZ1.

Unexpectedly, the C-terminal tail carrying the tyrosine-to-glutamic-acid mutation switched its orientation and interacted with PDZ2. To test the possibility that this switch blocked the peptide-binding pocket of PDZ2, we measured the binding affinities of a FITC-labeled, Tyr(-1)-to-glutamic-acid mutant C-peptide for PDZ1 and PDZ2. The mutant peptide showed no detectable binding to PDZ1; the K_d of the PDZ2-mutant C-peptide complex was 28 μ M, a value similar to the K_d of the wild-type C-peptide-PDZ2 complex. These results

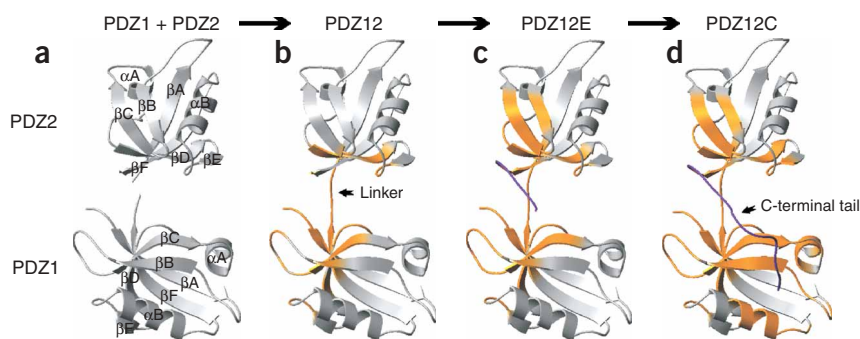


Figure 5 Supramolecular structural model of the autoinhibited conformation of X11 α PDZ12C. Each step of construct change resulted in backbone amide chemical shift changes with respect to the isolated PDZ1 and PDZ2. (a–c) The changes were sequentially mapped to the 3D structures of PDZ1 and PDZ2 (a). The structural models of PDZ12 (b) and PDZ12E (c) were constructed based on chemical shift changes induced by covalent linkage of the two PDZ domains using the isolated PDZ domain structures shown in Figure 3. (d) The structural model of PDZ12C was built by a simulated annealing protocol in CNS for NMR structure calculation. The PDZ1–C-peptide complex and PDZ2 structures were used as the starting point. The chemical shift changes of PDZ1 and PDZ2 were incorporated in the calculation as ambiguous distance restraints between the two domains³⁴.

indicate that phosphorylation of Tyr(-1) could act as a switch that regulates the opening and closing of the X11 PDZ domains. It remains to be established whether such a regulatory switch is indeed used in living cells.

To establish a correlation between the autoinhibited conformation of X11 α and the protein's potential function, we assayed the binding of the mutant PDZ domains to two known X11 α targets, neuronal calcium channels¹⁵ and presenilin^{13,14}. The X11 α mutant proteins used in this assay were the Tyr(-1)-to-glutamic-acid (Y836E) mutant, the Y836F mutant, a mutant with a disrupted PDZ1 ligand-binding pocket (Ile666, Leu667 and Gly668 in the GLFG loop all replaced by alanine), a mutant with a disrupted PDZ2 ligand-binding pocket (L759 and Gly760 in the GLGF loop both replaced by alanine) and a mutant with disruptions in the ligand-binding pockets of both PDZ domains. The Y836E mutant, which released the autoinhibited conformation of X11 α , enhanced the binding of both target proteins. In contrast, mutation of the target-binding pocket of PDZ1 (the PDZ1* and PDZ12* mutants) greatly weakened the binding of the two target proteins. As expected, the Y836F mutant had a target-binding property similar to that of the wild-type X11 α (Fig. 6).

DISCUSSION

The most important discovery of this study is that the highly conserved C-terminal tail of X11 α (and probably those of other X11 proteins) folds back and binds to the first PDZ domain of the PDZ tandem through intramolecular interactions, resulting in an autoinhibited conformation of X11 α . Thus, the target binding sites of PDZ domains are not always accessible. Substitution of the absolutely conserved Tyr(-1) with glutamate abolished the binding of the C-terminal tail to PDZ1 (Fig. 4), suggesting a possible regulatory mechanism of X11 by phosphorylation of the tyrosine residue. Further work is required to prove or refute the possibility that Tyr(-1) can indeed be phosphorylated. If Tyr(-1) is phosphorylated in cells, identification of the responsible tyrosine kinase(s) will help elucidate the regulatory mechanism of X11 proteins. Regulation of target-binding accessibility through an autoinhibitory mechanism may also be used by other proteins with PDZ domains. For example, the scaffold proteins Lnx1 and Lnx2 contain conserved PDZ-binding motifs (GTFL in Lnx1 and

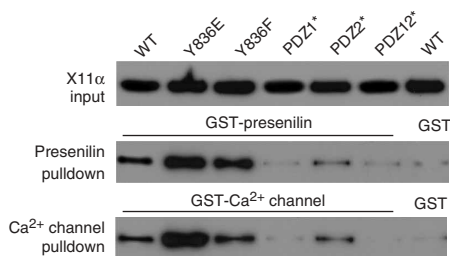


Figure 6 Correlation of the autoinhibited conformation of X11 α with the target-binding property of the protein. The C termini of presenilin (DQLAFHQFYI) and calcium channel (HHPDQDHW C) were fused to glutathione S-transferase, respectively. Purified recombinant GST fusion proteins were used for binding assays with wild-type (WT) X11 α and its various mutants, including Y836E, Y836F, PDZ1* (PDZ1 deficient in ligand binding), PDZ2* (PDZ2 deficient in ligand binding) and PDZ12* (PDZ2 with both its ligand binding sites disrupted). The amount of X11 α protein was detected by immunoblotting with antibody to c-Myc (9E10).

GSLV in Lnx2) at their extreme C-terminal ends. These motifs may interact with one or more PDZ domains within the Lnx proteins³¹. Given the promiscuity of the interactions between PDZ domains and their targets, it will also be important to confirm (by genetic or other approaches) whether the autoinhibited conformation discovered in our *in vitro* study is indeed used under cellular conditions.

This study also showed that PDZ1, PDZ2 and the entire C-terminal tail (PDZ12C) of X11 form an integral structural unit. PDZ12C has target-binding properties distinct from those of the three isolated domains or the simple sum of the three domains. The structural features of PDZ12C offer an explanation for the widely disparate observations of target binding by X11. First, our studies showed that the target-binding properties of individual PDZ domains cannot be directly translated to predict the properties of two domains acting in tandem in the intact protein. In particular, the tail-mediated autoinhibition of PDZ1 would occlude many C-terminal peptides from binding to the PDZ domain. Second, even though the binding pocket of PDZ2 is open in X11, its target binding can also be influenced by PDZ1 and the 16-residue tail. PDZ2 should therefore function properly only when the domain is attached to PDZ1 and the C-terminal peptide. This probably correlates with the observations that the binding of some X11 targets requires both PDZ domains^{13,14}. Because of these structural features of the X11 PDZ tandem, caution is necessary when interpreting biochemical binding data derived from truncation or mutation experiments. Synergistic interaction of two PDZ domains has also been observed in other proteins containing multiple PDZ domains, including the N-terminal PDZ tandem of PSD-95 (ref. 32), PDZ4 and PDZ5 of the glutamate receptor-interacting proteins³³ and the PDZ tandem of syntenin³⁴.

We also uncovered a distinct mode of PDZ domain-mediated target binding. The PDZ1 of X11 recognizes only the last two C-terminal amino acids of its targets, and the X11 PDZ1-binding C-terminal peptide does not form a β -strand as seen in the canonical PDZ-peptide complexes. The direct contact between the α A helix and the C-peptide indicates that the binding of a target to the PDZ domain can involve one or more regions outside the α B/ β B groove. It was recently shown that the binding of a C-terminal peptide from the interleukin-5 receptor to the PDZ2 of syntenin also involves only the last two hydrophobic amino acids of the peptide ligand³⁵. The interleukin-5 peptide binds to the PDZ2 of syntenin by forming an antiparallel β -sheet with the PDZ2 β B strand, largely because of the

open conformation of its α B/ β B groove (ref. 35). In contrast, the closed conformation of the α B/ β B groove of the X11 PDZ1 indicates that this domain is unlikely to be able to bind to C-terminal peptides using this conventional binding mode.

In summary, we have uncovered in X11 scaffold proteins an autoinhibited conformation of the PDZ tandem mediated by their highly conserved C termini. We further showed that the two PDZ domains and the entire C-terminal tail of X11 proteins function as a structural and functional supramodule. The autoinhibited conformation of X11 family members has the potential to be regulated by an as-yet-unknown mechanism possibly involving tyrosine phosphorylation. The identification of this regulatory mechanism will shed light on the functions of this highly conserved family of scaffold proteins.

METHODS

Expression and purification of proteins. PDZ1 (residues 655–747), PDZ12 (residues 655–822) and PDZ12C (residues 655–837) were PCR-amplified from the full-length gene encoding human X11 α and cloned into a modified pET32a vector³⁶. The resulting proteins contained a His₆-tag in their respective N termini. PDZ2 (residues 743–822) was cloned into another modified pET32a vector in which the nucleotides encoding the S-tag and thioredoxin were replaced by a DNA sequence encoding the B1 domain of streptococcal protein GB1. Proteins were expressed in BL21(DE3) *Escherichia coli* cells at 37 °C. The His-tagged PDZ proteins were purified by Ni-NTA agarose (Qiagen) affinity chromatography followed by size-exclusion chromatography. Uniformly ¹⁵N- and ¹⁵N/¹³C-labeled PDZ domains were prepared by growing bacteria in M9 minimal medium using ¹⁵NH₄Cl as the sole nitrogen source or ¹⁵NH₄Cl and ¹³C₆-glucose as the sole nitrogen and carbon sources, respectively. The NMR samples contained ~1.0 mM of PDZ proteins in 100 mM potassium phosphate at pH 6.5.

Nuclear magnetic resonance spectroscopy. NMR spectra were acquired at 30 °C on Varian Inova 500- or 750-MHz spectrometers. Backbone assignments were achieved using HNCOC, HNCACB and CBCA(CO)NH using ¹⁵N/¹³C-labeled samples^{37,38}. Nonaromatic, nonexchangeable side chain resonances were assigned using HCCH total correlation spectroscopy (HCCH-TOCSY) experiments. The side chains of aromatics were assigned by standard ¹H two-dimensional (2D) TOCSY/nuclear Overhauser effect spectroscopy (NOESY) experiments.

Structure calculations. Approximate interproton distance restraints were derived from ¹H 2D NOESY, 3D ¹⁵N-separated NOESY and 3D ¹³C-separated NOESY spectra. Intermolecular nuclear Overhauser effects (NOEs) between PDZ1 and the C-peptide were identified using a ¹³C-edited (F1), ¹³C/¹⁵N-filtered (F3) 3D NOESY spectrum on a ¹³C/¹⁵N-labeled PDZ1 in complex with unlabeled C-peptide³⁹. Hydrogen bonding restraints were generated from the standard secondary structure of the proteins. Backbone dihedral angle restraints were derived by the program TALOS⁴⁰. Structures were calculated using the program CNS⁴¹. The quality of the final 20 lowest energy structures was analyzed by PROCHECK_NMR⁴². The percentage of residues of the ensemble in the most favored, allowed and disallowed regions of the Ramachandran plot were 67.7, 32.3 and 0, respectively, for PDZ1; 69.0, 30.4 and 0.6 for the PDZ1–C-peptide complex; and 67.5, 31.7 and 0.8 for PDZ2.

C-terminal peptide ligand titration. C-terminal peptide ligand titrations of various PDZ domains were conducted by recording ¹H, ¹⁵N HSQC spectra of ¹⁵N-labeled protein samples (~0.2 mM) using commercially synthesized C-terminal peptides.

Fluorescence anisotropy measurements. Fluorescence anisotropy binding assays were performed on a PerkinElmer LS-55 fluorimeter equipped with an automated polarizer at 20 °C. FITC-labeled X11 α C-terminal peptide (FITC-EQPVYI) and its mutant version (FITC-EQPVEI) were commercially synthesized (GenScript) and were >95% pure. Fluorescence titration was performed

with increasing amounts of unlabeled PDZ proteins and constant amounts of FITC-labeled peptide (1 μ M). The titration curves were fitted with the MicroCal Origin software package.

Gel filtration chromatography. Analytical gel filtration chromatography was carried out on an AKTA FPLC system using a Superose 12 10/30 column (Amersham Pharmacia Biotech). Protein samples were dissolved in 50 mM Tris-HCl buffer (pH 7.5) in the presence of freshly dissolved DTT (1 mM).

Yeast two-hybrid assay. Yeast two-hybrid assays were done using Matchmaker System 3 (Becton Dickinson Biosciences). Briefly, PDZ1 was cloned into the pGBKT7 bait vector, and various PDZ domains or the C-terminal tail of X11 α were individually cloned into the pGADT7 prey vector. Protein interactions in the yeast two-hybrid assays were examined by cotransforming the engineered plasmids into competent yeast cells (AH109) and then plating the cells onto growth medium (DIFCO Laboratories) lacking leucine, tryptophan, adenine and histidine.

Illustrations. The figures were prepared using the programs MOLMOL⁴³, MOLSCRIPT⁴⁴, Raster3D⁴⁵ and GRASP (<http://trantor.bioc.columbia.edu/grasp/>).

Accession codes. Protein Data Bank codes: The coordinates of PDZ1, PDZ1 in complex with the C-peptide, and PDZ2 have been deposited under the accession codes 1U37, 1U38 and 1U39, respectively.

Note: Supplementary information is available on the Nature Structural & Molecular Biology website.

ACKNOWLEDGMENTS

This work was supported by grants CERG and AOE/B-15/01 from the University Grants Committee of Hong Kong to N.Y.I., J.X. and M.Z. The NMR spectrometer used in this work was purchased with funds donated to the Biotechnology Research Institute by the Hong Kong Jockey Club. M.Z. and N.Y.I. were recipients of the Croucher Foundation Senior Research Fellowship. We thank H. Zheng for the presenilin expression construct.

COMPETING INTERESTS STATEMENT

The authors declare that they have no competing financial interests.

Received 28 February; accepted 2 June 2005

Published online at <http://www.nature.com/nsmb/>

- Duclos, F. *et al.* Gene in the region of the Friedreich ataxia locus encodes a putative transmembrane protein expressed in the nervous system. *Proc. Natl. Acad. Sci. USA* **90**, 109–113 (1993).
- Okamoto, M. & Sudhof, T.C. Mints, Munc18-interacting proteins in synaptic vesicle exocytosis. *J. Biol. Chem.* **272**, 31459–31464 (1997).
- Borg, J.P., Yang, Y., De Taddeo-Borg, M., Margolis, B. & Turner, R.S. The X11 α protein slows cellular amyloid precursor protein processing and reduces A β 40 and A β 42 secretion. *J. Biol. Chem.* **273**, 14761–14766 (1998).
- McLoughlin, D.M., Irving, N.G. & Miller, C.C. The Fe65 and X11 families of proteins: proteins that interact with the Alzheimer's disease amyloid precursor protein. *Biochem. Soc. Trans.* **26**, 497–500 (1998).
- Biederer, T. & Sudhof, T.C. Mints as adaptors. Direct binding to neurexins and recruitment of munc18. *J. Biol. Chem.* **275**, 39803–39806 (2000).
- McLoughlin, D.M. *et al.* Mint2/X11-like colocalizes with the Alzheimer's disease amyloid precursor protein and is associated with neuritic plaques in Alzheimer's disease. *Eur. J. Neurosci.* **11**, 1988–1994 (1999).
- Okamoto, M. & Sudhof, T.C. Mint 3: a ubiquitous mint isoform that does not bind to munc18-1 or -2. *Eur. J. Cell Biol.* **77**, 161–165 (1998).
- Borg, J.P. *et al.* Molecular analysis of the X11-mLin-2/CASK complex in brain. *J. Neurosci.* **19**, 1307–1316 (1999).
- Tomita, S. *et al.* Interaction of a neuron-specific protein containing PDZ domains with Alzheimer's amyloid precursor protein. *J. Biol. Chem.* **274**, 2243–2254 (1999).
- Borg, J.P., Ooi, J., Levy, E. & Margolis, B. The phosphotyrosine interaction domains of X11 and FE65 bind to distinct sites on the YENPTY motif of amyloid precursor protein. *Mol. Cell Biol.* **16**, 6229–6241 (1996).
- McLoughlin, D.M. & Miller, C.C. The intracellular cytoplasmic domain of the Alzheimer's disease amyloid precursor protein interacts with phosphotyrosine-binding domain proteins in the yeast two-hybrid system. *FEBS Lett.* **397**, 197–200 (1996).
- Zhang, Z. *et al.* Sequence-specific recognition of the internalization motif of the Alzheimer's amyloid precursor protein by the X11 PTB domain. *EMBO J.* **16**, 6141–6150 (1997).
- Biederer, T., Cao, X., Sudhof, T.C. & Liu, X. Regulation of APP-dependent transcription complexes by Mint/X11s: differential functions of Mint isoforms. *J. Neurosci.* **22**, 7340–7351 (2002).
- Lau, K.F., McLoughlin, D.M., Standen, C. & Miller, C.C. X11 α and x11 β interact with presenilin-1 via their PDZ domains. *Mol. Cell Neurosci.* **16**, 557–565 (2000).
- Maximov, A., Sudhof, T.C. & Bezprozvanny, I. Association of neuronal calcium channels with modular adaptor proteins. *J. Biol. Chem.* **274**, 24453–24456 (1999).
- Stricker, N.L. & Huganir, R.L. The PDZ domains of mLin-10 regulate its trans-Golgi network targeting and the surface expression of AMPA receptors. *Neuropharmacology* **45**, 837–848 (2003).
- Mueller, H.T., Borg, J.P., Margolis, B. & Turner, R.S. Modulation of amyloid precursor protein metabolism by X11 α /Mint-1. A deletion analysis of protein-protein interaction domains. *J. Biol. Chem.* **275**, 39302–39306 (2000).
- Kaech, S.M., Whitfield, C.W. & Kim, S.K. The LIN-2/LIN-7/LIN-10 complex mediates basolateral membrane localization of the C. elegans EGF receptor LET-23 in vulval epithelial cells. *Cell* **94**, 761–771 (1998).
- Rongo, C., Whitfield, C.W., Rodal, A., Kim, S.K. & Kaplan, J.M. LIN-10 is a shared component of the polarized protein localization pathways in neurons and epithelia. *Cell* **94**, 751–759 (1998).
- Whitfield, C.W., Benard, C., Barnes, T., Hekimi, S. & Kim, S.K. Basolateral localization of the *Caenorhabditis elegans* epidermal growth factor receptor in epithelial cells by the PDZ protein LIN-10. *Mol. Biol. Cell* **10**, 2087–2100 (1999).
- Butz, S., Okamoto, M. & Sudhof, T.C. A tripartite protein complex with the potential to couple synaptic vesicle exocytosis to cell adhesion in brain. *Cell* **94**, 773–782 (1998).
- Setou, M., Nakagawa, T., Seog, D.H. & Hirokawa, N. Kinesin superfamily motor protein KIF17 and mLin-10 in NMDA receptor-containing vesicle transport. *Science* **288**, 1796–1802 (2000).
- Guillaud, L., Setou, M. & Hirokawa, N. KIF17 dynamics and regulation of NR2B trafficking in hippocampal neurons. *J. Neurosci.* **23**, 131–140 (2003).
- Ho, A., Morishita, W., Hammer, R.E., Malenka, R.C. & Sudhof, T.C. A role for Mints in transmitter release: Mint 1 knockout mice exhibit impaired GABAergic synaptic transmission. *Proc. Natl. Acad. Sci. USA* **100**, 1409–1414 (2003).
- Songyang, Z. *et al.* Recognition of unique carboxyl-terminal motifs by distinct PDZ domains. *Science* **275**, 73–77 (1997).
- Zhang, M. & Wang, W. Organization of signaling complexes by PDZ-domain scaffold proteins. *Acc. Chem. Res.* **36**, 530–538 (2003).
- Sheng, M. & Sala, C. PdZ domains and the organization of supramolecular complexes. *Annu. Rev. Neurosci.* **24**, 1–29 (2001).
- Harris, B.Z. & Lim, W.A. Mechanism and role of PDZ domains in signaling complex assembly. *J. Cell Sci.* **114**, 3219–3231 (2001).
- Birrane, G., Chung, J. & Ladias, J.A.A. Novel mode of ligand recognition by the erbin PDZ domain. *J. Biol. Chem.* **278**, 1399–1402 (2003).
- Kang, B.S. *et al.* PDZ tandem of human syntenin. Crystal structure and functional properties. *Structure* **11**, 459–468 (2003).
- Sollerbrant, K. *et al.* The Coxsackievirus and adenovirus receptor (CAR) forms a complex with the PDZ domain-containing protein ligand-of-numb protein-X (LNX). *J. Biol. Chem.* **278**, 7439–7444 (2003).
- Long, J.F. *et al.* Supramolecular structure and synergistic target binding of the N-terminal tandem PDZ domains of PSD-95. *J. Mol. Biol.* **327**, 203–214 (2003).
- Feng, W., Shi, Y., Li, M. & Zhang, M. Tandem PDZ repeats in glutamate receptor-interacting proteins have a novel mode of PDZ domain-mediated target binding. *Nat. Struct. Biol.* **10**, 972–978 (2003).
- Zimmermann, P. *et al.* Characterization of syntenin, a syndecan-binding PDZ protein, as a component of cell adhesion sites and microfilaments. *Mol. Biol. Cell* **12**, 339–350 (2001).
- Kang, B.S., Cooper, D.R., Devedjiev, Y., Derewenda, U. & Derewenda, Z.S. Molecular roots of degenerate specificity in syntenin's PDZ2 domain: reassessment of the PDZ recognition paradigm. *Structure* **11**, 845–853 (2003).
- Feng, W., Fan, J.S., Jiang, M., Shi, Y.W. & Zhang, M. PDZ7 of glutamate receptor interacting protein binds to its target via a novel hydrophobic surface area. *J. Biol. Chem.* **277**, 41140–41146 (2002).
- Bax, A. & Grzesiek, S. Methodological advances in protein NMR. *Acc. Chem. Res.* **26**, 131–138 (1993).
- Kay, L.E. & Gardner, K.H. Solution NMR spectroscopy beyond 25 kDa. *Curr. Opin. Struct. Biol.* **7**, 722–731 (1997).
- Zwahlen, C. *et al.* Methods for measurement of intermolecular NOEs by multinuclear NMR spectroscopy: application to a bacteriophage N-peptide/boxB RNA complex. *J. Am. Chem. Soc.* **119**, 6711–6721 (1997).
- Cornilescu, G., Delaglio, F. & Bax, A. Protein backbone angle restraints from searching a database for chemical shift and sequence homology. *J. Biomol. NMR* **13**, 289–302 (1999).
- Brunger, A.T. *et al.* Crystallography & NMR system: a new software suite for macromolecular structure determination. *Acta Crystallogr. D Biol. Crystallogr.* **54**, 905–921 (1998).
- Laskowski, R.A., Rullmann, J.A., MacArthur, M.W., Kaptein, R. & Thornton, J.M. AQUA and PROCHECK-NMR: programs for checking the quality of protein structures solved by NMR. *J. Biomol. NMR* **8**, 477–486 (1996).
- Koradi, R., Billeter, M. & Wuthrich, K. MOLMOL: a program for display and analysis of macromolecular structures. *J. Mol. Graph.* **14**, 51–55 (1996).
- Kraulis, P.J. MOLSCRIPT: a program to produce both detailed and schematic plots of protein structures. *J. Appl. Crystallogr.* **24**, 946–950 (1991).
- Merritt, E. & Murphy, M. Raster3D version 2.0. A program for photorealistic molecular graphics. *Acta Crystallogr. D Biol. Crystallogr.* **50**, 869–873 (1994).